Virology 382 (2008) 83–90

Contents lists available at ScienceDirect

Virology

journal homepage: www.elsevier.com/locate/yviro

Stacking interactions of W271 and H275 of SeMV serine protease with W43 of natively unfolded VPg confer catalytic activity to protease

Smita Nair [a], P. Gayathri [b], M.R.N. Murthy [b], H.S. Savithri [a,*]

[a] Department of Biochemistry, Indian Institute of Science, Bangalore–560012, Karnataka State, India
[b] Molecular Biophysics Unit, Indian Institute of Science, Bangalore–560012, India

ARTICLE INFO

Article history:
Received 27 June 2008
Returned to author for revision 16 July 2008
Accepted 15 August 2008
Available online 7 October 2008

Keywords:
Sesbania mosaic virus
Serine protease
VPg
Natively unfolded protein
Aromatic residues
Histidine
Stacking interactions
Positive CD peak

ABSTRACT

N-terminal serine protease domain of *Sesbania mosaic virus* polyprotein, requires fused VPg for its activity. W43 of VPg mediates aromatic stacking interactions (characterized by 230 nm positive CD peak) with protease. A stretch of aromatic residues (F269, W271, Y315, and Y319) exposed in the protease domain were mutated to identify the interacting partner of W43. W271A Protease-VPg mutant showed absence of cleavage activity both *in vivo* and in *trans*, with concomitant loss of the 230 nm CD peak. F269A Protease-VPg mutant was partially active. Mutations of the tyrosines did not result in loss of protease activity or the CD peak. Interestingly, H275, though not a part of the exposed aromatic stretch, was shown to be essential for protease activity and contributed significantly to the CD peak. Hence, we conclude that W271 and H275 of the protease domain mediate aromatic stacking interactions with W43 of VPg thereby rendering the protease active.

Introduction

Sesbania mosaic virus (SeMV), a member of the genus *Sobemovirus*, is a ssRNA virus infecting *Sesbania grandiflora* (Lokesh et al., 2001). Its genome of 4149 nucleotides in length is linked at its 5′ end to a viral protein genome linked (VPg) and includes four ORFs. The two central ORFs 2a and 2b are translated into polyproteins. ORF 2b is translated by −1 ribosomal frameshift mechanism into polyprotein with a domain arrangement of protease-VPg-RNA dependent RNA polymerase. Both polyproteins 2a and 2b are processed into functional domains by their N-terminal serine protease domain. The *cis* and *trans* catalytic activities of the protease domain were demonstrated earlier (Satheshkumar et al., 2004). The protease cleaves the polyprotein at specific Glu-Thr/Ser residues. The crystal structure of SeMV serine protease domain was determined at 2.4 Å resolution (Gayathri et al., 2006). The protease domain exhibited the characteristic trypsin fold and was found to be closer to the cellular serine proteases than to the other viral proteases. H298, T279, and N308 were identified to be the residues in S1 binding pocket. Importance of these residues in the activity of serine protease was established by mutational analysis (Gayathri et al., 2006).

In SeMV, VPg is a 77 amino acid long protein. It was shown earlier that the fused VPg domain plays an important role in the *cis* and *trans* catalytic activity of the protease (Satheshkumar et al., 2005). *In vitro* studies demonstrated that purified protease domain was incapable of carrying out proteolysis in *trans* as opposed to the protease-VPg fusion protein. Bioinformatics and biophysical studies revealed that VPg is a "natively unfolded" protein (Satheshkumar et al., 2005). Tryptophan at position 43 of VPg was shown to mediate aromatic stacking interaction with the protease, which resulted in a positive peak at 230 nm in the Far-UV CD spectrum of protease-VPg fusion protein. Mutation of W43 in VPg to phenylalanine abrogated the protease activity in *cis* and *trans* with the concomitant loss of the 230 nm CD peak. The current study involves identification of the residues in the protease domain that mediate aromatic stacking interactions with W43 of VPg and thereby rendering the protease active.

The positive CD peak at 230 nm has been mainly attributed to the contribution from tryptophans and tyrosines (Lacadena et al., 1995; Schechter et al., 1971; Woody, 1994). Also, clustering of tyrosine and phenylalanine side chains has been suggested as an explanation for the unusual Far-UV CD spectra, especially in proteins with low α-helical content (Freskgard et al., 1994). The crystal structure of SeMV protease domain revealed a stretch of aromatic amino acids exposed to the solvent. These residues, F269, W271, Y315 and Y319 are not consecutive in the sequence, but form a stack near the C-terminus of

Abbreviations: SeMV, *Sesbania mosaic virus*; ssRNA, single-stranded RNA; ORF, open reading frame; VPg, viral protein genome linked; SDM, site-directed mutagenesis; PV, ΔN-118 Protease-VPg; CD, Circular dichroism.

* Corresponding author. Fax: +91 80 2360 0814.
E-mail address: bchss@biochem.iisc.ernet.in (H.S. Savithri).

0042-6822/$ – see front matter © 2008 Elsevier Inc. All rights reserved.
doi:10.1016/j.virol.2008.08.034

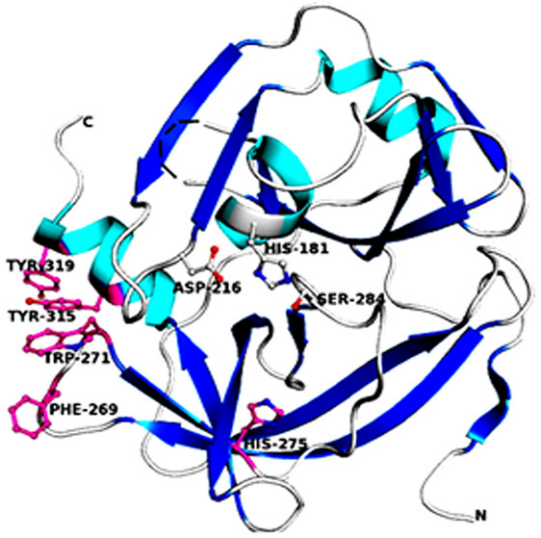

Fig. 1. Ribbon diagram of SeMV protease domain. Shows the exposed aromatic amino acids F269, W271, Y315 and Y319 and H275 of S1 binding pocket. Active site residues S284, H181 and D216 are also shown. The disordered residues in the structure are represented by broken lines.

the protein (Fig. 1). Residues F269 and W271 are present in the loop joining the bll and cll β-strands and residues Y315 and Y319 form part of the C-terminal helix (Gayathri et al., 2006). The sequence analysis of the protease domain from all the known sobemoviruses shows the presence of a conserved His at position 275 (Fig. 1). A study with histidine as an interacting aromatic partner using 1271 non-redundant His–X pairs revealed that 37% pairs were involved in interactions with aromatic partner less than 6 residues apart (Meurissea et al., 2003; Samanta et al., 1999; Thomas et al., 2002). In mammalian microsomal apo-cytochrome C, neighboring histidine and tryptophan residues are involved in π-stacking interactions (Wang et al., 2006). The structure and interaction studies of His37 and Trp41 of the M2 ion channel of Influenza A virus, suggest a model in which the channel is opened by a His37–Trp41 cation-π interaction (Takeuchi et al., 2003). Histidine–tryptophan interactions have also been studied in the case of Barnase enzyme, Murine interleukin-6, and Cathepsin S, where such interactions have a role in protein stability, activity etc. (Brömme et al., 1996; Loewenthal et al., 1992; Matthews et al., 1997). Therefore, along with the exposed aromatic residues (F269, W271, Y315, and Y319), H275 was also targeted for mutagenesis as a possible residue involved in aromatic interactions with W43 of VPg.

In this paper we have identified residues W271 and H275 of the protease, but not the tyrosines to be important for interactions with W43 of the VPg domain. Only these residues were found to contribute significantly to the 230 nm CD peak. F269A mutant was partially active and also showed the positive CD peak.

Results

Generation of mutations in the protease domain

The residues of the aromatic stretch F269, W271, Y315, Y319 and H275 were mutated to phenylalanine or alanine by PCR-based SDM approach as described in Materials and methods section. All the mutations were generated in ΔN-118 Protease-VPg (PV) template. The active site residues of the protease and the cleavage site between protease and VPg were intact in these constructs. In order to purify the PV and its aromatic residue mutants, the cleavage site residue E325 was mutated to A as described in Materials and methods. However, E325A mutant of PV-H275A was not generated, as intact PV-H275A could be purified.

Expression of the mutants and analysis of the protease activity in vivo

PV and its mutants were expressed in *E. coli* BL21 (DE3) pLys S cells. The *in vivo* cleavage by protease domain was monitored by running the total induced cell extract on 12% SDS-PAGE followed by western blot analysis with antiprotease antibodies. As shown in Fig. 2, PV underwent almost complete cleavage to give 26 kDa ΔN-118 protease (Pro) band and VPg (Fig. 2, lane 1). The band corresponding to VPg was not detected with antiprotease antibodies. PV-W271F mutant was only partially active and hence both the 34 kDa PV and 26 kDa Pro bands were detected (Fig. 2, lane 2). On the other hand, PV-W271A mutant showed complete absence of the Pro band (Fig. 2, lane 3), suggesting that no cleavage had occurred in this case. Interestingly, PV-H275A mutant also showed complete absence of the 26 kDa Pro band (Fig. 2, lane 5). PV-F269A mutant exhibited partial activity as evident from the presence of both 34 kDa PV and 26 kDa Pro bands (Fig. 2, lane 4). The PV-Y315A mutant got cleaved completely whereas PV-Y319A mutant was nearly completely cleaved to give 26 kDa Pro band (Fig. 2, lane 6, 8). As expected no bands were detected in the uninduced lane (Fig. 2, lane 7). The *in vivo* cleavage assay indicates that W271 and H275 are absolutely essential for the protease activity.

trans Cleavage assay

The PV-S284A (PVSA), PV-E325A (PVEA) and PVEA mutants were expressed and purified as mentioned in Materials and methods. The PVEA-Y315A mutant precipitated during dialysis and therefore could not be used for any further studies. The protease active site residue mutant PVSA was used as the substrate and PVEA, the cleavage site mutant was used as an enzyme. PVSA (substrate) was incubated with increasing amounts of purified PVEA or PVEA mutants (enzyme) and analyzed on 15% SDS-PAGE. PVEA and PVEA-Y319A were similarly active and cleaved the substrate, as evident from the presence of both Pro and VPg bands (Fig. 3). On the other hand, PVEA-W271A mutant was almost inactive as it was barely able to cleave the substrate PVSA in *trans* (Fig. 3). Also, PV-H275A mutant was completely inactive (Fig. 3). PVEA-W271F and PVEA-F269A mutants were only partially active as evident from the presence of uncleaved PVSA (Fig. 3) (compare first lane of PVEA-W271F and PVEA-F269A with PVEA).

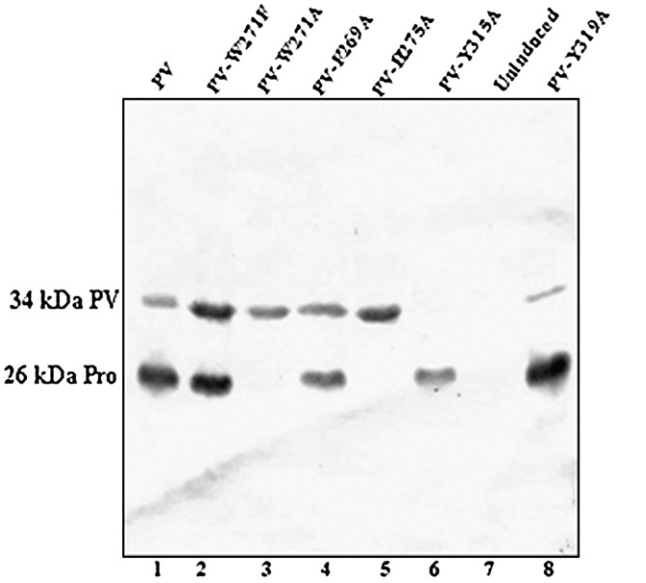

Fig. 2. *In vivo* cleavage assay. PV and the mutants PV-W271F, PV-W271A, PV-F269A, PV-H275A, PV-Y315A, and PV-Y319A were expressed in *E. coli* BL21 (DE3) pLys S cells and analyzed on 12% SDS-PAGE followed by western analysis using polyclonal antibodies to the protease domain as the primary antibody.

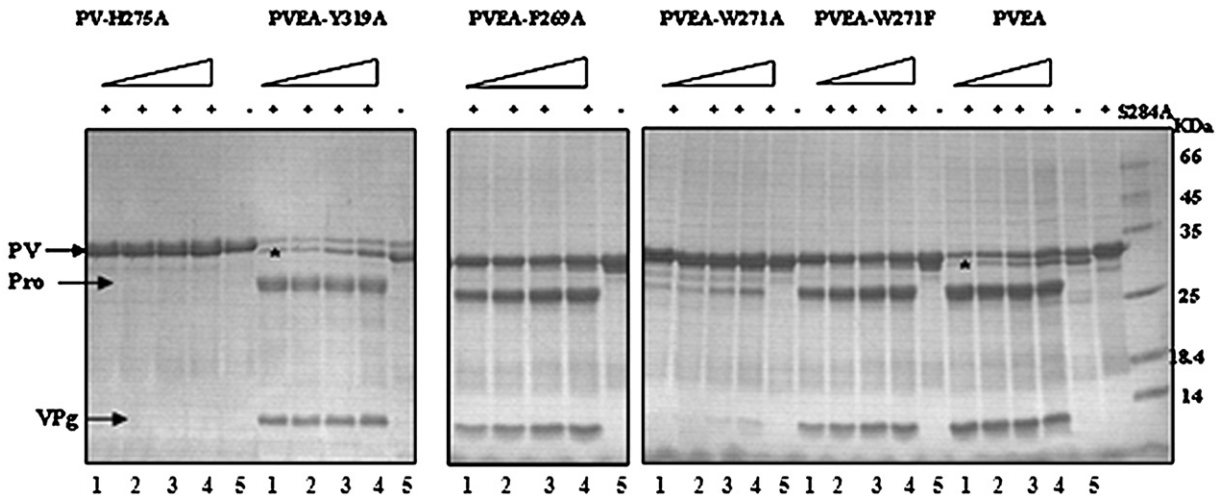

Fig. 3. *trans* Cleavage assay. 20 μg of purified PVSA (substrate) was incubated with increasing amounts of purified PVEA or PVEA mutants (enzyme) (1.25 μg, 2.5 μg, 5 μg and 10 μg) in 20 mM Tris buffer pH-8.0 for 2 h at 37 °C. The cleavage products were analyzed on 15% SDS-PAGE. Lanes indicated as − have no PVSA added and 10 μg of respective PVEA. * denotes band due to cleavage of PVEA at an additional site.

However, as both substrate and enzyme had the same molecular mass, it was difficult to estimate the degree of partial activity. These results suggest that in *trans* as well, the activity of the protease domain particularly depends on W271 and H275, but not at all on the tyrosine residue Y319.

Far-UV CD spectral analysis

The Far-UV CD spectra of the protease-VPg fusion protein showed the presence of a positive peak at 230 nm that was absent from the spectra of either protease or VPg alone (Satheshkumar et al., 2005). W43 of VPg was shown to contribute directly to this positive peak. In order to assess the role of F269, W271, H275 and Y319 in the aromatic stacking interactions, considered to be responsible for the 230 nm positive peak, Far-UV CD spectra were obtained for PVEA and the mutants. As expected, PVEA gave a positive peak at 230 nm (Fig. 4). Similar positive peak was also observed for PVEA-Y319A mutant suggesting that the aromatic interactions were intact in this mutant (Fig. 4). However, the positive peak at 230 nm was completely absent from the spectra of both PVEA-W271A and PV-H275A mutants (Fig. 4). Both PVEA-W271F and PVEA-F269A showed reduced positive ellipticity at 230 nm but the former showed greater decrease in positive ellipticity as compared to the latter (Fig. 4). The presence/absence of the positive peak indeed correlated well with the activity profile of the mutants. These results suggest that of the four aromatic residues of the protease domain that are exposed to the solvent, in the protease-

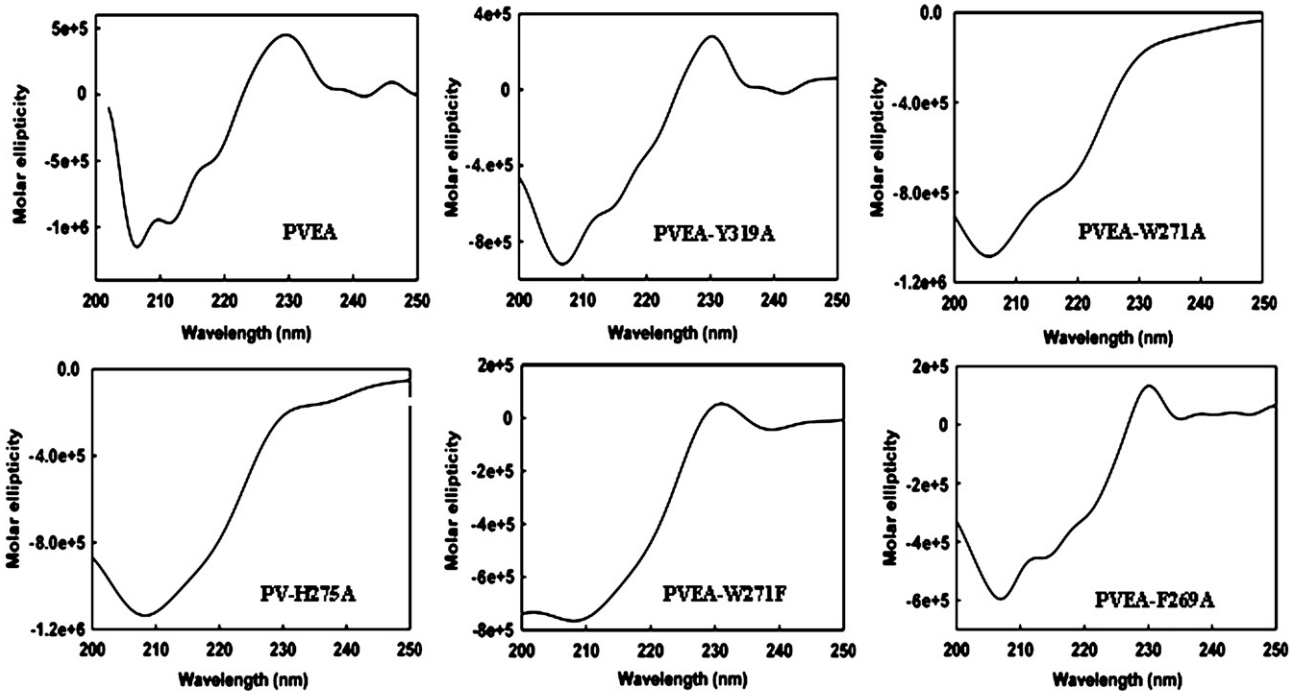

Fig. 4. Far-UV CD spectra. The Far-UV circular dichroism experiments on PVEA and the mutants were carried out using a Jasco-815 spectropolarimeter. The ellipticity was monitored at 25 °C from 200 nm to 250 nm using 0.2 mg/ml of the purified protein in 20 mM Tris pH 8.0.

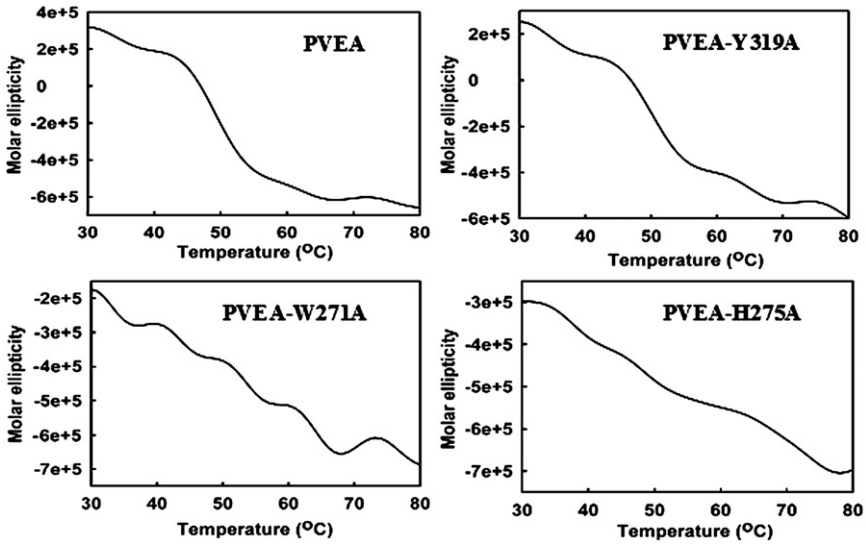

Fig. 5. Thermal denaturation studies. The thermal denaturation of PVEA and the mutants was carried out using a Peltier Thermo Cycler. 0.2 mg/ml of the purified protein in 20 mM Tris pH 8.0 was heated from 30 °C to 80 °C. The change in molar ellipticity at 230 nm was monitored with the change in temperature.

VPg fusion protein, only W271 contributes to the 230 nm CD peak significantly and hence also to the stacking interaction with W43 of VPg. Interestingly, though H275 is not a part of the exposed aromatic residues in the protease domain, it appears to be involved in the stacking interactions with W43 of VPg.

Thermal denaturation studies

Effect of temperature on the positive CD at 230 nm observed for PVEA can be an index of the thermal stability of the aromatic stacking interactions between protease and VPg domains. Therefore, the CD change was measured as a function of temperature at 230 nm at which the positive peak is observed. A sharp decrease was observed in the molar ellipticity values at 230 nm from 43 °C and the melting was nearly complete by 56 °C (Fig. 5). Thus, the melting curve obtained with PVEA could fit into a two state model in which the transition from state A (aromatic stacking interactions intact) to state B (complete loss in aromatic stacking interactions) was concerted or cooperative. From the first derivative graph of molar ellipticity at 230 nm Vs temperature curve, a T_m (temperature at which 50% of the molecules have lost the aromatic stacking interactions) of 50 °C was determined. PVEA-Y319A mutant also showed a similar transition with increase in temperature (Fig 5) and the T_m was calculated to be 51 °C. However, for mutants PVEA-W271A and PV-H275A no such transition was observed, suggestive of a non-cooperative melting. This is consistent with the fact that the aromatic interactions were already disrupted in these mutants (Fig. 5). PVEA-W271F and PVEA-F269A on the other hand had lower positive CD at 230 nm and they exhibited a T_m of 45 °C and 46 °C, respectively (data not shown), suggesting that in these mutants weakened stacking interactions were responsible for the decrease in melting temperature.

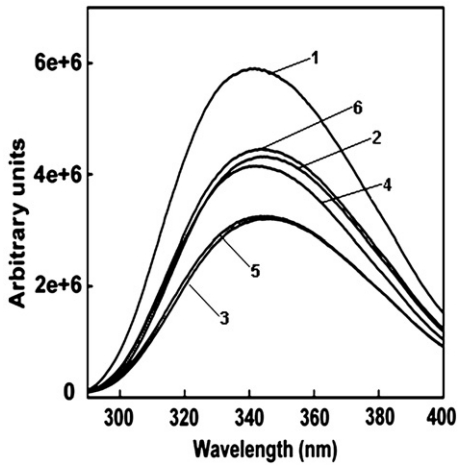

Fig. 6. Fluorescence spectra. The fluorescence measurements of PVEA and the mutants were carried out using a Perkin Elmer Life Science LS-55 spectrofluorimeter. 0.1 mg/ml of protein in 20 mM Tris pH 8.0 was excited at 280 nm and the emission was measured from 290 nm to 400 nm. Curves 1, 2, 3, 4, 5 and 6 correspond to the fluorescence spectra of PVEA, PVEA-W271F, PVEA-W271A, PVEA-F269A, PV-H275A and PVEA-Y319A respectively.

Intrinsic fluorescence

The intrinsic fluorescence spectra of PVEA and the mutants were obtained to monitor the changes in the environment of aromatic residues (if any). For a folded globular protein in which the aromatic residues are present in a hydrophobic environment the emission maximum (λ_{max}) is expected to be in the range of 330 nm–345 nm. Upon exposure of the aromatic residues to the solvent the λ_{max} gets red shifted (Eftink, 2000). ΔN-118 protease has five tryptophans, five tyrosines and six phenylalanines. VPg has two tyrosines, three tryptophans and three phenylalanines. The fluorescence spectrum of PVEA showed an emission maximum of 341 nm (Fig. 6, curve 1, Table 1), suggesting that most of the aromatic residues in the protease-VPg fusion protein were buried. The emission maxima of PVEA-W271A and PV-H275A were red shifted to 346 nm and 345 nm, respectively (Fig. 6, curves 3 and 5, Table 1). The PVEA-W271F mutant showed a λ_{max} of 345 nm (Fig. 6, curve 2, Table 1). The red shift in the emission spectra indicated the exposure of the tryptophans to the solvent in these mutants and possible destabilization of the aromatic

Table 1
Emission maxima

Pro-VPg	λ_{max}
1. PVEA	341
2. PVEA-W271F	345
3. PVEA-W271A	346
4. PVEA-F269A	342
5. PV-H275A	345
6. PVEA-Y319A	343

The emission maxima (λ_{max}) of PVEA and the mutants.

stacking interactions with W43 of VPg. However, the λ_{max} for PVEA-F269A and PVEA-Y319A did not change significantly and were 342 nm and 343 nm, respectively (Fig. 6, curves 4 and 6, Table 1).

In general, the fluorescence intensities of the mutants were lower when compared to PVEA. This could be because of the loss of the aromatic residues due to mutation or due to a change in the environment of the aromatic residues resulting in the quenching of fluorescence. The later possibility is unlikely in the case of PVEA-Y319A and PVEA-F269A mutants as there was no change in their λ_{max} values.

Gel filtration analysis

In order to see if the disruption of the aromatic interactions between protease and VPg also affected the oligomeric status of the fusion protein, gel filtration analysis was carried out. PVEA and its mutants were subjected to FPLC on an analytical Superdex S-200 column. As shown in Fig. 7, PVEA eluted as a major monomer peak and a minor dimer peak. Both these peaks were earlier reported to exhibit protease activity and 230 nm positive CD peak (Satheshkumar et al., 2005). PVEA-W271A and PV-H275A that exhibited complete loss of activity both *in vivo* and in *trans* and the absence of 230 nm positive CD peak, showed elution profiles different from PVEA. PVEA-W271A eluted as monomer and dimer peaks, almost equal in ratio (Fig. 7). Interestingly, there was also a peak eluting near the void volume of the column. Also, PV-H275A mutant also eluted as monomer and dimer peaks along with a major peak near the void volume.

In the case of PVEA-W271F that exhibited very small positive peak at 230 nm and partial activity, almost equal size monomer and dimer peaks were observed along with a peak near the void volume. PVEA-F269 eluted as monomer and dimer peaks along with a small peak near the void volume. These results suggest that in the absence of aromatic interactions, the unfolded VPg would cause the protease-VPg to elute abnormally and cause aggregation.

Discussion

The N-terminal serine protease domain of SeMV polyprotein is responsible for the polyprotein processing (Satheshkumar et al., 2004). However, the protease is not active when expressed alone but active when expressed as N-terminal fusion to VPg, a natively unfolded protein. The two domains were proposed to be involved in aromatic interactions that conferred activity to the protease (Satheshkumar et al., 2005). The structure of protease revealed a stack of aromatic residues exposed to the solvent (Fig. 1). Site-directed mutants of residues F269, W271, Y315 and Y319 were generated to identify their role in mediating the interactions and hence the activity of protease. H275, though not a part of exposed aromatic stack in the protease, was chosen for mutational analysis as it lies close to the W271 in sequence and is conserved in the protease domain across all the known sobemoviruses. The *in vivo* and *trans* cleavage assays suggested that residues W271 and H275 but not Y315 or Y319 are crucial for protease activity (Fig. 2, lanes 3, 5, 6, and 8 and Fig. 3). PVEA-W271F and PVEA-F269A mutants were partially active (Fig. 2, lane 2, 4 and Fig. 3). The activity of PVEA-W271F mutant could be accounted for in terms of the conservative nature of replacement of W by F. When the sequences of all sobemoviral proteases were analyzed, the position 271 was occupied in 3 cases by W, in 2 by Y, in another 2 by F (Dwyer et al., 2003; Lee and Anderson, 1998; Lokesh et al., 2001; Makinen et al., 1995; Othman and Hull, 1995; Wu et al., 1987; Yassi et al., 1994). This suggests that such conservative replacements have already been tolerated across other sobemoviral proteases. However, the significance of VPg and its aromatic interactions on the protease activity remains to be established in other sobemoviruses. F269 however, is not a conserved residue and therefore may have only an indirect effect on the activity of the protease.

The Far-UV CD spectrum of protease-VPg is characterized by a positive peak at 230 nm (Satheshkumar et al., 2005). Spectral analysis of the aromatic mutants showed that W271 and H275, but not F269 and Y319 are the major contributors of the 230 nm positive peak as there was a complete loss in the positive peak only for PVEA-W271A and PV-H275A mutants (Fig. 4). Unlike some of the proteins where clustering of aromatic residues contributes to their unusual Far-UV CD spectra (Day, 1973; Freskgard et al., 1994; Lacadena et al., 1995; Vuilleumier et al., 1993), it is interesting to note that in SeMV protease, though aromatic residues F269, W271, Y315 and Y319 appear to form a stack near the C-terminus, the Far-UV CD spectrum of the protease

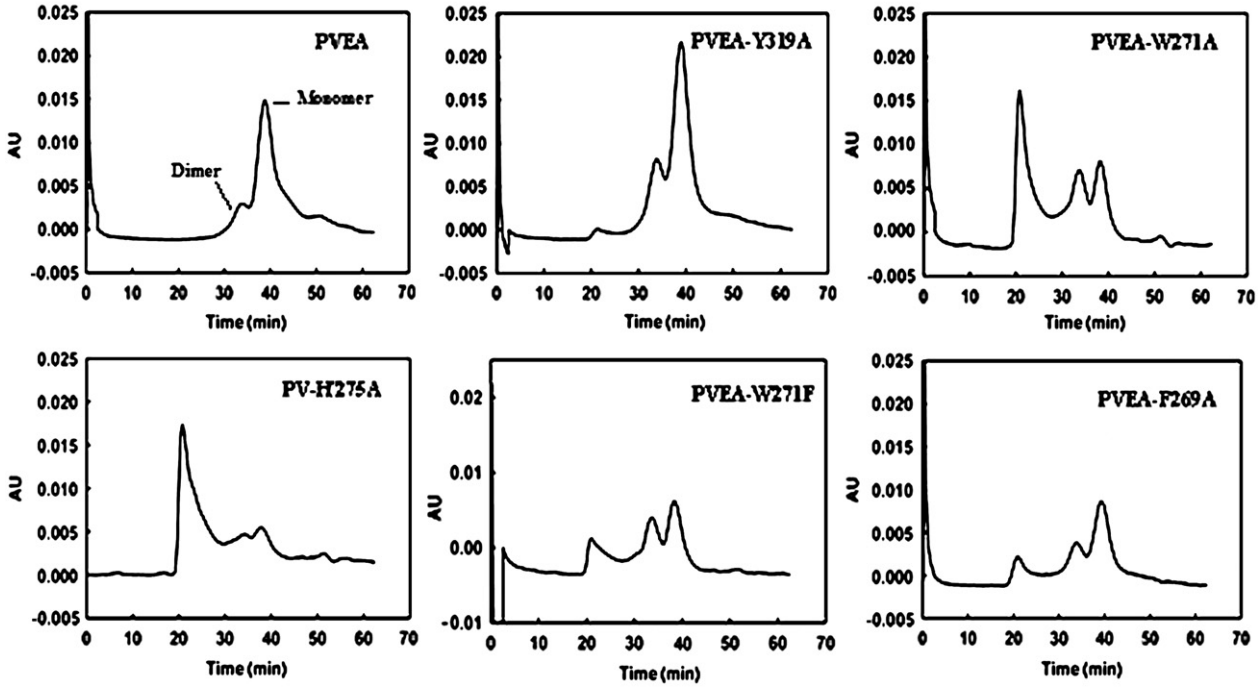

Fig. 7. Gel filtration analysis. PVEA and the mutants were analyzed on a FPLC system (Amersham Biosciences) using a Superdex S-200 analytical gel filtration column.

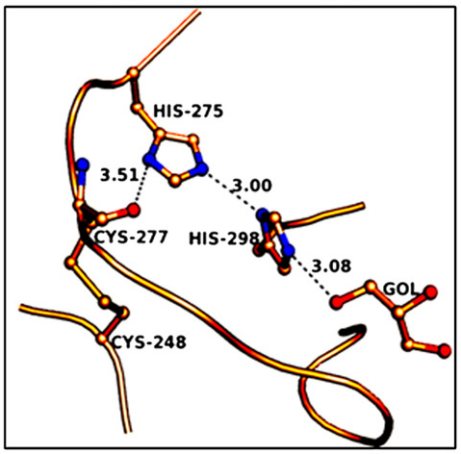

Fig. 8. Shows the relay of H-bond (represented by dotted lines) between H298 and H275 and C277.

lacks the positive peak at 230 nm. The stacking interactions of W43 of VPg with W271 and H275 of protease in protease-VPg is what contributes to the positive CD peak at 230 nm and hence to the protease activity. Also, the partial activity and reduced positive CD peak of PVEA-F269A mutant (Fig. 2 lane 4, Fig. 3 and Fig. 4) suggests a supportive but not a direct role of this residue in the stacking interactions. F269, due to its close proximity to W271 may aid in positioning the later for the interactions. However, the possibility of other interactions between protease and VPg domain, especially at their C- and N-terminus respectively, that would bring the natively unfolded VPg close to the protease domain to mediate aromatic stacking interactions cannot be ruled out.

The thermal stability of the aromatic interactions was monitored by the change in ellipticity at 230 nm as a function of temperature. Unlike PVEA and PVEA-Y319A that showed cooperative melting, PVEA-W271A and PV-H275A exhibited absence of cooperative melting, reconfirming that in the latter cases the aromatic interactions had been completely disrupted (Fig. 5). Intrinsic fluorescence measurements have been used as a handle for monitoring the disruption of interacting interfaces. In Triosephosphate isomerase from *Plasmodium flaciparum*, the interface residue Y74 when mutated to G led to the destabilization of the subunit interface as suggested by the 3 nm shift in the emission maxima of the mutant (Maithal et al., 2002). Intrinsic fluorescence measurements were determined for PVEA and its mutants. As shown in Fig. 6 and Table 1, there was a decrease in the fluorescence intensities and a significant shift of 5 nm and 4 nm, respectively, in the λ_{max} of PVEA-W271A and PV-H275A mutants as compared to PVEA. This suggests that the mutations have indeed led to the disruption of the aromatic stacking interactions. For PVEA-W271F mutant that was partially active and had a greatly reduced positive CD peak (Fig. 2 lane 2, Fig. 3 and Fig. 4), a similar red shift in λ_{max} was observed indicating weakened aromatic interactions in this mutant. PVEA-F269A and PVEA-Y319A did not show any significant shift in the λ_{max} (Table 1).

It is interesting to note that in the protease domain, unlike the other aromatic residues studied, H275 does not form part of the exposed stack. The crystal structure of the protease domain shows that H275 faces the substrate binding pocket. In the protease, the S1 binding site residue H298 is directed towards the active site and H-bonds with the substrate glutamate. The Nδ1 of H298 forms H-bond with Nε2 of H275 (Fig. 8). The conformation of H275 side chain is in turn stabilized by the H-bond from Nδ1 to the main chain N of the disulphide bonded C277, thereby generating a relay of H-bonds. A relay of H-bonds between a His triad was proposed to stabilize the charge on the substrate glutamate in the *Streptomyeces grieses* serine protease (Nienaber et al., 1993; Stennicke et al., 1996).

As evident from the results presented in the paper, mutation of H275 to A results in the loss of activity and the positive CD peak at 230 nm (Fig. 2, lane 5; Fig. 3 and Fig. 4). These observations suggest that in protease-VPg, H275 is probably not involved in H-bonding network that could stabilize the charge on the substrate. It is possible that, in the active protease-VPg fusion protein, H275 is a part of the aromatic stack with W271 and interacts with W43 of VPg, thereby rendering the protease active. In the absence of these interactions i.e. in the inactive protease domain, it could assume an unproductive conformation and get stably H-bonded in the substrate binding pocket (Fig. 8). A similar side chain flipping was observed for the active site residue His 47 of glutamyl endopeptidase from *Bacillus intermedius* (Meijers et al., 2004).

The crystal structure of protease shows a well formed active site and an oxyanion hole (Gayathri et al., 2006). Yet the protease requires VPg as its C-terminal fusion to be catalytically active. Also, addition of purified VPg in *trans* to the protease does not render it active (Satheshkumar et al., 2005). This suggests that only in the fusion the two domains can interact to bring about conformational changes in the protease so that it can now cleave the substrate. The significance of conformational changes introduced in the protease as a result of its stacking interaction with VPg becomes more relevant in the *in vivo* scenario. The free protease domain released from protease-VPg following processing, will remain inactive with its H275 assuming an unproductive conformation in the absence of stacking interactions. This would lead to the temporal regulation of the processing of the polyproteins which may be crucial for efficient multiplication of the virus. The results presented in the paper clearly suggest that W271 and H275 of SeMV protease domain are involved in stacking

Table 2
List of primers

Name	5′ to 3′ sequence	Description
Pro F269A-s	CAACTTCTGAGGCTACTTGGAAGTTGACCCAC	Primers used for F269A mutation in the protease domain. HinCII site abolished is underlined.
Pro F269A-a	GTGGGTCAATTTCCAAGTAGCCTCAGAAGTT	
Pro W271F-s	CAACTTCTGAGTTTACTGCGAAGTTGACCCAC	Primers used for W271F mutation in the protease domain. HinCII site abolished is underlined.
Pro W271F-a	GTGGGTCAATTTCGCAGTAAACTCAGAAGTT	
Pro W271A-s	CTTCTGAATTCACTGCGAAGTTGACCCACACC	Primers used for W271A mutation in the protease domain. EcoRI site created is underlined.
Pro W271A-a	GGTGTGGGTCAACTTCGCAGTGAATTCAGAAG	
Pro H275A-s	GAGTTTACTTGGAAATTGACCGCCACCTGTCCTAC	Primers used for the H275A mutation in the protease domain. HinCII site abolished is underlined.
Pro H275A-a	GTAGGACAGGTGGCGGTCAATTTCCAAGTAAACTC	
Pro Y315A-s	GTTAACATGTTCGCTGTTGCGAATTAC	Primers used for Y315A mutation in the protease domain. KspAI site created is underlined.
Pro Y315A-a	GTAATTCGCAACAGCGAACATGTTAAC	
Pro Y319A-s	CTATGTTGCGAATGCCCTCTTGAGGTCTAATG	Primers used for Y319A mutation in the protease domain. AflII site abolished is underlined.
Pro Y319A-a	CATTAGACCTCAAGAGGGCATTCGCAACATAG	
Pro-VPg-E325A-s	CTCTTAAGATCTAATGCGACTCTCCC	Primers used for E325A mutation in the protease domain. BglII site created is underlined.
Pro-VPg-E325A-a	GGGAGAGTCGCATTAGATCTTAAGAG	

Shows the primers used for mutagenesis. s—sense primer; a—antisense primer.

interactions with W43 of VPg domain. Thus, histidine–aromatic stacking interactions between protease and a natively unfolded protein play crucial role in conferring the activity to the protease.

Materials and methods

The fine chemicals used for biochemical and molecular biological work were purchased from Sigma, Calbiochem and Novagen. Restriction endonucleases and DNA modification enzymes and polymerases were purchased from New England Biolabs and MBI Fermentas. All the other chemicals used were of analytical grade.

Oligonucleotide primers

The oligonucleotide primers used for site-directed mutagenesis (SDM) were custom made from Sigma Chemicals (Table 2).

Expression and purification

The recombinant clones of protease-VPg were transformed in *E. coli* BL21 DE3 pLys S cells and the proteins were expressed by inducing the culture with 0.3 mM IPTG for 12 h at 16 °C. The cell pellet was resuspended in the sonication buffer (50 mM Tris pH 8.0, 200 mM NaCl, 0.2% Triton X-100, 5% glycerol), sonicated and the expression was checked by SDS-polyacrylamide gel electrophoresis (PAGE) (Laemmli, 1970). All the protease-VPg fusion proteins (cleavage site mutant PVEA, active site mutant PVSA, aromatic residue mutants) were purified from the soluble fraction by Ni-NTA affinity chromatography (Novagen). The purity of the protein was checked on SDS-PAGE.

Site-directed mutagenesis

PCR-based site-directed mutagenesis (SDM) was carried out using overlapping sense and antisense primers with desired changes in the bases (Weiner et al., 1994) (Table 2). Restriction sites were incorporated into the primers for easy screening of the mutant clones. The PCR was carried out using High Fidelity Phusion polymerase (New England Biolabs) with appropriate primers and template. The PCR product was digested with DpnI enzyme to remove the template, following which it was transformed into *E. coli* DH5α cells. The plasmids were isolated from the colonies and screened for mutation by restriction digestion and the mutations were confirmed by DNA sequencing.

trans Cleavage assay

ΔN-118 Protease-VPg S284A (PVSA), with its active site residue mutated was not capable of auto catalysis and hence could be used as substrates for *trans* cleavage assay. The ΔN-118 Protease-VPg E325A (PVEA) with its cleavage site residue mutated could only recognize the substrate in *trans* and hence was used as an enzyme. Both the constructs were expressed and purified as mentioned above. The *trans* cleavage assay was performed by incubating increasing amounts (1.25 μg, 2.5 μg, 5 μg and 10 μg) of purified PVEA (enzyme) with 20 μg of purified PVSA (substrate) in 20 mM Tris pH 8.0 for 2 h at 37 °C. The cleavage products were analyzed on 15% SDS-PAGE.

Circular dichroism spectroscopy

The CD spectra were recorded using a Jasco-815 spectropolarimeter. The ellipticity was monitored at 25 °C from 200 nm to 250 nm using 0.2 mg/ml of the purified protein in 20 mM Tris pH 8.0. A scan speed of 50 nm/min, 0.2 cm path length cuvette, band width of 1 nm and response time of 1 s were used. The spectra were averaged for 3 scans and corrected with buffer blanks. The molar ellipticity was calculated using the software provided by the manufacturer.

The thermal denaturation studies were carried out using a Peltier Thermo Cycler. 0.2 mg/ml of the purified protein in 20 mM Tris pH 8.0 was heated from 30 °C to 80 °C. The change in molar ellipticity at 230 nm was monitored as a function of temperature to obtain the thermal melting curve. The T_m was determined by plotting a first derivative graph of molar ellipticity Vs temperature. The temperature corresponding to the peak of the graph was taken as T_m (temperature at which 50% of the molecules had lost stacking interactions due to melting).

Fluorescence spectroscopy

The fluorescence measurements were carried out using Perkin Elmer Life Science LS-55 spectrofluorimeter. 0.1 mg/ml of protein in 20 mM Tris pH 8.0 was excited at 280 nm and the emission was measured from 290 nm to 400 nm. Excitation and emission band-pass was kept as 5 nm.

Gel filtration analysis

Oligomeric status of the PVEA and its mutants was analyzed on a FPLC system (Amersham Biosciences) using a Superdex S-200 analytical gel filtration column. The column was precalibrated with standards of known molecular mass. From the retention time the elution volume was calculated and the molecular masses of the samples were estimated from the standard graph.

Acknowledgments

HSS and MRNM thank the Council of Scientific and Industrial Research (CSIR) and the Department of Biotechnology (DBT) of the Government of India for financial support. SN acknowledges the Indian Institute of Science, Bangalore for fellowship.

References

Brömme, D., Bonneau, P.R., Purisima, E., Lachance, P., Hajnik, S., Thomas, D.Y., Storer, A.C., 1996. Contribution to activity of histidine–aromatic, amide–aromatic, and aromatic–aromatic interactions in the extended catalytic site of cysteine proteinases. Biochemistry 35, 3970–3979.

Day, L.A., 1973. Circular dichroism and ultraviolet absorption of a deoxyribonucleic acid binding protein of filamentous bacteriophage. Biochemistry 12 (26), 5329–5339.

Dwyer, G.I., Njeru, R., Williamson, S., Fosu-Nyarko, J., Hopkins, R., Jones, R.A., Waterhouse, P.M., Jones, M.G., 2003. The complete nucleotide sequence of Subterranean clover mottle virus. Arch. Virol. 148 (11), 2237–2247.

Eftink, M.R., 2000. Intrinsic fluorescence of proteins. In: Lacowitz, J.R. (Ed.), Topics in Fluorescence Spectroscopy, Vol 6. Kluwer Academic, New York, pp. 1–16.

Freskgard, P.O., Martensson, L.G., Jonasson, P., Jonsson, B.H., Carlsson, U., 1994. Assignment of the contribution of the tryptophan residues to the circular dichroism spectrum of human carbonic anhydrase II. Biochemistry 33 (47), 14281–14288.

Gayathri, P., Satheshkumar, P.S., Prasad, K., Nair, S., Savithri, H.S., Murthy, M.R.N., 2006. Crystal structure of the serine protease domain of *Sesbania* mosaic virus polyprotein and mutational analysis of residues forming the S1-binding pocket. Virology 346 (2), 440–451.

Lacadena, J., Martı'nez, d.P.A., Gasset, M., Patin, B., Campos-Olivas, R., Va'zquez, C., Martı'nez-Riz, A., Manchen, J.M., On, aderra, M., Gavilanes, J.G., 1995. Characterization of the antifungal protein secreted by the mould *Aspergillus giganteus*. Arch. Biochem. Biophys. 324 (2), 273–281.

Laemmli, U.K., 1970. Cleavage of structural proteins during the assembly of the head of bacteriophage T4. Nature 227 (259), 680–685.

Lee, L., Anderson, E.J., 1998. Nucleotide sequence of a resistance breaking mutant of southern bean mosaic virus. Arch. Virol. 143 (11), 2189–2201.

Loewenthal, R., Sanchot, J., Fersht, A.R., 1992. Histidine–aromatic interactions in barnase elevation of histidine p*K*, and contribution to protein stability. J. Mol. Biol. 224, 759–770.

Lokesh, G.L., Gopinath, K., Satheshkumar, P.S., Savithri, H.S., 2001. Complete nucleotide sequence of *Sesbania* mosaic virus: a new virus species of the genus *Sobemovirus*. Arch. Virol. 146 (2), 209–223.

Maithal, K., Ravindra, G., Nagaraj, G., Singh, S.K., Balaram, H., Balaram, P., 2002. Subunit interface mutation disrupting an aromatic cluster in *Plasmodium falciparum* triosephosphate isomerase: effect on dimer stability. Protein Eng. 15 (7), 575–584.

Makinen, K., Tamm, T., Naess, V., Truve, E., Puurand, U., Munthe, T., Saarma, M., 1995. Characterization of cocksfoot mottle sobemovirus genomic RNA and sequence comparison with related viruses. J. Gen. Virol. 76, 2817–2825.

Matthews, J.M., Ward, L.D., Hammacher, A., Norton, R.S., Simpson, R.J., 1997. Roles of histidine 31 and tryptophan 34 in the structure, self-association, and folding of murine interleukin-6. Biochemistry 36, 6187–6196.

Meijers, R., Blagova, E.V., Levdikov, V.M., Rudenskaya, G.N., Chestukhina, G.G., Akimkina, T.V., Kostrov, S.V., Lamzin, V.S., Kuranova, I.P., 2004. The crystal structure of glutamyl endopeptidase from *Bacillus intermedius* reveals a structural link between zymogen activation and charge compensation. Biochemistry 43 (10), 2784–2791.

Meurissea, R., Brasseura, R., Thomas, A., 2003. Aromatic side-chain interactions in proteins. near- and far-sequence His–X pairs. Biochim. Biophys. Acta 1649, 85–96.

Nienaber, V.L., Breddam, K., Birktoft, J.J., 1993. A glutamic acid specific serine protease utilizes a novel histidine triad in substrate binding. Biochemistry 32 (43), 11469–11475.

Othman, Y., Hull, R., 1995. Nucleotide sequence of the bean strain of southern bean mosaic virus. Virology 206 (1), 287–297.

Samanta, U., Debnath, P., Chakrabarti, P., 1999. Packing of aromatic rings against tryptophan residues in proteins. Acta Crystallogr. D 55, 1421–1427.

Satheshkumar, P.S., Lokesh, G.L., Savithri, H.S., 2004. Polyprotein processing: *cis* and *trans* proteolytic activities of *Sesbania* mosaic virus serine protease. Virology 318 (1), 429–438.

Satheshkumar, P.S., Gayathri, P., Prasad, K., Savithri, H.S., 2005. "Natively unfolded" VPg is essential for *Sesbania* mosaic virus serine protease activity. J Biol Chem 280 (34), 30291–30300.

Schechter, B., Schechter, I., Ramachandran, J., Conway-Jacobs, A., Sela, M., 1971. The synthesis and circular dichroism of a series of peptides possessing the structure (L-tyrosyl-L-alanyl-L-glutamyl)n. Eur. J. Biochem. 20 (3), 301–308.

Stennicke, R.H., Birktoft, J.J., Breddam, K., 1996. Characterization of the S1 binding site of the glutamic acid-specific protease from *Streptomyces griseus*. Protein Sci. 5, 2266–2275.

Takeuchi, H., Okada, A., Miura, T., 2003. Roles of the histidine and tryptophan side chains in the M2 proton channel from influenza A virus. FEBS Lett. 552, 35–38.

Thomas, A., Meurisse, R., Charloteaux, B., Brasseur, R., 2002. Aromatic side-chain interactions in proteins. I. Main structural features. Proteins 48, 628–634.

Vuilleumier, S., Sancho, J., Loewenthal, R., Fersht, A.R., 1993. Circular dichroism studies of barnase and its mutants: characterization of the contribution of aromatic side chains. Biochemistry 32, 10303–10313.

Wang, L., Sun, N., Terzyan, S., Zhang, X., Benson, D.R., 2006. A histidine/tryptophan π-stacking interaction stabilizes the heme-independent folding core of microsomal apocytochrome b5 relative to that of mitochondrial apocytochrome b5. Biochemistry 45, 13750–13759.

Weiner, M.P., Costa, G.L., Schoettlin, W., Cline, J., Mathur, E., Bauer, J.C., 1994. Site-directed mutagenesis of double-stranded DNA by the polymerase chain reaction. Gene 151 (1–2), 119–123.

Woody, R.W., 1994. Contributions of tryptophan side chains to the far-ultraviolet circular dichroism of proteins. Eur. Biophys. J. 23 (4), 253–262.

Wu, S.X., Rinehart, C.A., Kaesberg, P., 1987. Sequence and organization of southern bean mosaic virus genomic RNA. Virology 161 (1), 73–80.

Yassi, M.N., Ritzenthaler, C., Brugidou, C., Fauquet, C., Beachy, R.N., 1994. Nucleotide sequence and genome characterization of rice yellow mottle virus RNA. J. Gen. Virol. 75, 249–257.